AN EFFICIENT RPIM FOR SIMULATING WAVE MOTIONS IN SATURATED POROUS MEDIA

S.L. Chen[1,2] and Y.X. Li[1]

[1] *Dept. of Civil Engineering, Nanjing University of Aeronautics and Astronautics, Nanjing, China*
[2] *Dept. of Earthquake Engineering , Institute of Engineering Mechanics, Harbin. China*
Email:iemcsl@yahoo.com.cn

ABSTRACT :

An efficient meshless technique for simulating wave motions in saturated porous media is introduced in this paper. Using radial point interpolation method (RPIM) and considering the precision requirement in wave motion simulation, a lumped-mass RPIM for saturated porous media with clear physical concepts is derived. Combining explicit time integration with the lumped-mass RPIM leads to a decoupled radial point interpolation method (decoupled RPIM) for dynamic analysis without solving algebra equation set. A two-dimensional problem is calculated by the proposed decoupled RPIM, the ordinary RPIM， and the finite element method (FEM). The accuracy and efficiency of these methods are compared, which demonstrate that the proposed decoupled RPIM has comparable accuracy with the ordinary RPIM and the finite element method, but has high efficiency in simulating wave motions in saturated porous media.

KEYWORDS: saturated porous media, meshless method, radial point interpolation method, explicit integration scheme

1. INTRODUCTION

Porous media consists of a solid phase, usually referred to as a matrix or skeleton, as well as closed and open pores. Examples of porous media are soils, rocks, the human bone, et al. The mechanics of porous media is of utmost relevance in many disciplines in engineering and science, such as geotechnical engineering, biomechanics, and materials science. In geotechnical earthquake engineering, multiphase dynamics plays a major role in the prediction of the local site response where the buildup of fluid pressure induced by seismic shaking could lead to a rapid loss of strength of the saturated soil deposit, a phenomenon commonly called as liquefaction. A fluid-filled porous medium theory was proposed by Biot (1941) to analyze this transient response. Most of the transient response problems are solved by numerical methods such as finite element method (FEM) and finite difference method (FDM) in conjunction with appropriate time integration schemes. Typical FEM methods were proposed by Ghaboussi and Wilson(1972), Zienkiewicz and Shiomi (1984), Provost(1985), Sandhu and Hong(1987), Yiagos and Prevost(1991), Diebels and Ehlers(1996), Huang et al.(2004). However, it is difficult for FEM to analyze the problems associated with moving boundary and large deformation. Recently developed meshless methods could overcome these disadvantages because meshless methods do not use any element.

In recent years, meshless methods have achieved remarkable progress. A group of meshless methods have been developed including smooth particle hydrodynamics (SPH) (Gingold and Monaghan,1977), diffuse element method (DEM) (Nayroles et al.,1992), element free Galerkin (EFG) method (Belytschko et al.,1994), reproducing kernel particle method(RKPM) (Liu et al.,1995), the meshless local petrov-Galerkin (MLPG) method (Atluri and Zhu,1998), the local point interpolation method (LPIM) (Gu and Liu, 2001), the radial point interpolation method (RPIM) (Wang and Liu,2001), and the local radial point interpolation method (LRPIM) (Liu and Gu 2001).

Wang (2001,2002) discusses the numerical solution of Biot's consolidation theory using the PIM method and RPIM method. Karim et al.(2002) analyzed transient response of saturated porous elastic soil under cyclic loading using EFG method. The RPIM is advantageous over the meshless methods based on moving least square (MLS) method in implementation of essential boundary condition and over the PIM with polynomial basis in avoiding singularity when shape functions are constructed. However, the present RPIM used for

dynamics needs to solve algebra equation sets at each time step, and the efficiency is very low, which prevent the RPIM to solve large scale problem in engineering. So, we need to find a meshless method which is not only accurate but also efficient.

In this paper, an efficient RPIM method is proposed for the transient response of saturated porous media. This paper is organized as follows. First, the governing equations for fluid-saturated elastic porous media are described. Then its weak form is developed. Considering the precision requirement in wave motion simulation, a lumped-mass RPIM with clear physical concept is derived. Explicit time integration is employed, which combined with the lumped-mass RPIM leads to dynamic analysis without solving algebra equation set. Finally, a two-dimensional problem is calculated by the proposed RPIM, the ordinary RPIM and the FEM, and the accuracy and efficiency are compared.

2. MATHEMATICAL MODEL

2.1. Governing Differential Equations

In this paper, we mainly introduce a decoupling technique, which is not limited to any specific model. So, without loss of generality, the model introduced by Men (1982) is selected. Its equations are reformulated as:

For the solid skeleton:

$$\mathbf{L}_s^T\boldsymbol{\sigma}' - (1-n)\mathbf{L}_w^T P + b(\dot{\mathbf{U}} - \dot{\mathbf{u}}) = (1-n)\rho_s\ddot{\mathbf{u}} \tag{2.1}$$

For the pore fluid:

$$-n\mathbf{L}_w^T P + b(\dot{\mathbf{u}} - \dot{\mathbf{U}}) = n\rho_w\ddot{\mathbf{U}} \tag{2.2}$$

Compatibility conditions(assuming that the initial pore pressure and initial volumetric strain are zero)：

$$-nP = E_w[ne^w + (1-n)e^s] \tag{2.3}$$

The isotropic linear elastic constitutive law for solid skeleton and the relation between strain and displacement are

$$\boldsymbol{\sigma}' = \mathbf{D}\mathbf{e} \qquad e^s = \mathbf{L}_w\mathbf{u} \tag{2.4}$$

$$\mathbf{e} = \mathbf{L}_s\mathbf{u} \qquad e^w = \mathbf{L}_w\mathbf{U} \tag{2.5}$$

Where, $\mathbf{L}_s$ and $\mathbf{L}_w$ are differential operator matrix, $\boldsymbol{\sigma}'$ and P are the effective stress and the fluid pressure respectively, $\mathbf{U}$ and $\mathbf{u}$ are the displacements of the fluid and solid skeleton respectively, ρ_s and ρ_w represent the densities of the solid skeleton and fluid respectively, n is porosity and b is defined as $b = n^2/k$， where k is the permeability coefficient of the pore fluid. E_w is the bulk modulus of the pore fluid，e^s and e^w denote the volumetric strains of the solid skeleton and pore fluid respectively, $\mathbf{e}$ is the solid strain tensor，$\mathbf{D}$ is the matrix of material constants.

Substituting Eqns.2.3-2.5into Eqn.2.1 and Eqn.2.2 respectively, one obtains equilibrium equations in term of $\mathbf{U}$ and $\mathbf{u}$.

$$\mathbf{L}_s^T\mathbf{D}\mathbf{L}_s\mathbf{u} + \frac{(1-n)}{n}\mathbf{L}_w^T E_w\left[n\mathbf{L}_w\mathbf{U} + (1-n)\mathbf{L}_w\mathbf{u}\right] + b(\dot{\mathbf{U}} - \dot{\mathbf{u}}) = (1-n)\rho_s\ddot{\mathbf{u}} \tag{2.6}$$

$$\mathbf{L}_w^T E_w\left[n\mathbf{L}_w\mathbf{U} + (1-n)\mathbf{L}_w\mathbf{u}\right] + b(\dot{\mathbf{u}} - \dot{\mathbf{U}}) = n\rho_w\ddot{\mathbf{U}} \tag{2.7}$$

2.2. Boundary Conditions

The governing Eqn.2.6and Eqn.2.7must be complemented with boundary conditions

$$\mathbf{u}-\bar{\mathbf{u}}=\mathbf{0} \qquad \mathbf{U}-\bar{\mathbf{U}}=\mathbf{0} \tag{2.8}$$

where, $\bar{\mathbf{u}}$ and $\bar{\mathbf{U}}$ are, respectively, the prescribed displacements of solid and fluid phase on the boundary Γ_D.

$$\hat{\mathbf{n}}\boldsymbol{\sigma}-\bar{\mathbf{t}}=\mathbf{0} \qquad (P-\bar{P})\mathbf{n}=\mathbf{0} \tag{2.9}$$

where, $\boldsymbol{\sigma}$ is the average stress vector of the solid phase, its tensor form is $\sigma_{ij}=\sigma'_{ij}-(1-n)P\delta_{ij}$, δ_{ij} is Kronecker delta function. $\bar{\mathbf{t}}$ and $\bar{P}$ are, respectively, the prescribed average traction of the solid phase and the pore fluid pressure on the Γ_N, the vector $\mathbf{n}$ is the unit outward normal to the boundary Γ_N, $\hat{\mathbf{n}}$ is a matrix with unit outward normal components as its elements.

3. GALERKIN WEAK FORM

The weighted residual forms of the Eqn.2.6and Eqn.2.7have the following forms

$$\int_\Omega \mathbf{W}_I^T\left(\mathbf{L}_s^T\mathbf{D}\mathbf{L}_s\mathbf{u}+\frac{(1-n)}{n}\mathbf{L}_w^T\mathbf{E}_w\left[n\mathbf{L}_w\mathbf{U}+(1-n)\mathbf{L}_w\mathbf{u}\right]\right)dV$$
$$+\int_\Omega \mathbf{W}_I^T\left(b(\dot{\mathbf{U}}-\dot{\mathbf{u}})-(1-n)\rho_s\ddot{\mathbf{u}}\right)dV=0 \tag{3.1}$$

$$\int_\Omega \mathbf{W}_I^T\left(\mathbf{L}_w^T E_w\left[n\mathbf{L}_w\mathbf{U}+(1-n)\mathbf{L}_w\mathbf{u}\right]+b(\dot{\mathbf{u}}-\dot{\mathbf{U}})-n\rho_w\ddot{\mathbf{U}}\right)dV=0 \tag{3.2}$$

Where, W_I is the weight function at node I.

In order to obtain the discretized system equations, the global problem domain Ω is represented by properly distributed field nodes. Using the RPIM shape function, we can approximate the trial function for the displacement at a point $\mathbf{x}$ as

$$\mathbf{u}(\mathbf{x},t)=\sum_{J=1}^{N}\boldsymbol{\Phi}_J\mathbf{u}_J \qquad \mathbf{U}(\mathbf{x},t)=\sum_{J=1}^{N}\boldsymbol{\Phi}_J\mathbf{U}_J \tag{3.3}$$

where, N is the number of nodes in the support domain of a sampling point at $\mathbf{x}$, and $\boldsymbol{\Phi}_J$ is the matrix of shape functions of node J, $\mathbf{u}_J$ and $\mathbf{U}_J$ are the nodal displacements.

Substituting Eqn.3.3 into Eqn.3.1 and Eqn.3.2, we can obtain:

$$\int_\Omega \mathbf{W}_I^T\left(\mathbf{L}_s^T\mathbf{D}\mathbf{L}_s\sum_{J=1}^{N}\boldsymbol{\Phi}_J\mathbf{u}_J+\frac{(1-n)}{n}\mathbf{L}_w^T\mathbf{E}_w\left[n\mathbf{L}_w\sum_{J=1}^{N}\boldsymbol{\Phi}_J\mathbf{U}_J+(1-n)\mathbf{L}_w\sum_{J=1}^{N}\boldsymbol{\Phi}_J\mathbf{u}_J\right]\right)d\Omega$$
$$+\int_\Omega \mathbf{W}_I^T\left(b\sum_{J=1}^{N}\boldsymbol{\Phi}_J(\dot{\mathbf{U}}_J-\dot{\mathbf{u}}_J)-(1-n)\rho_s\sum_{J=1}^{N}\boldsymbol{\Phi}_J\ddot{\mathbf{u}}_J\right)d\Omega=0 \tag{3.4}$$

$$\int_\Omega \mathbf{W}_I^T\mathbf{L}_w^T E_w\left(n\mathbf{L}_w\sum_{J=1}^{N}\boldsymbol{\Phi}_J\mathbf{U}_J+(1-n)\mathbf{L}_w\sum_{J=1}^{N}\boldsymbol{\Phi}_J\mathbf{u}_J\right)d\Omega$$
$$+\int_\Omega \mathbf{W}_I^T\left(b\sum_{J=1}^{N}\boldsymbol{\Phi}_J(\dot{\mathbf{u}}_J-\dot{\mathbf{U}}_J)-n\rho_w\sum_{J=1}^{N}\boldsymbol{\Phi}_J\ddot{\mathbf{U}}_J\right)d\Omega=0 \tag{3.5}$$

Integrating the first term on the left hand side of Eqn.3.5 and Eqn.3.6 by parts, and considering $\mathbf{W}_I = \mathbf{\Phi}_I$ for Galerkin method, we can obtain

$$\sum_{J=1}^{N}\mathbf{M}_{IJ}^{s}\ddot{\mathbf{u}}_J + \sum_{J=1}^{N}\mathbf{K}_{IJ}^{ss}\mathbf{u}_J + \sum_{J=1}^{N}\mathbf{K}_{IJ}^{sw}\mathbf{U}_J + \sum_{J=1}^{N}\mathbf{C}_{IJ}^{ss}\dot{\mathbf{u}}_J + \sum_{J=1}^{N}\mathbf{C}_{IJ}^{sw}\dot{\mathbf{U}}_J = \mathbf{F}_I^{s} \tag{3.6}$$

$$\sum_{J=1}^{N}\mathbf{M}_{IJ}^{w}\ddot{\mathbf{U}}_J + \sum_{J=1}^{N}\mathbf{K}_{IJ}^{ws}\mathbf{u}_J + \sum_{J=1}^{N}\mathbf{K}_{IJ}^{ww}\mathbf{U}_J + \sum_{J=1}^{N}\mathbf{C}_{IJ}^{ws}\dot{\mathbf{u}}_J + \sum_{J=1}^{N}\mathbf{C}_{IJ}^{ww}\dot{\mathbf{U}}_J = \mathbf{F}_I^{w} \tag{3.7}$$

Where the nodal mass matrices are equal to

$$\mathbf{M}_{IJ}^{s} = \int_{\Omega}\mathbf{\Phi}_I^T(1-n)\rho_s\mathbf{\Phi}_J d\Omega \qquad \mathbf{M}_{IJ}^{w} = \int_{\Omega}\mathbf{\Phi}_I^T n\rho_w\mathbf{\Phi}_J d\Omega \tag{3.8}$$

The nodal damping matrices, representing the viscous coupling between both phases, are given by

$$\mathbf{C}_{IJ}^{ss} = \int_{\Omega}\mathbf{\Phi}_I^T b\mathbf{\Phi}_J d\Omega \qquad \mathbf{C}_{IJ}^{sw} = \mathbf{C}_{IJ}^{ws} = -\mathbf{C}_{IJ}^{ww} = -\mathbf{C}_{IJ}^{ss} \tag{3.9}$$

The nodal stiffness matrices are expressed as

$$\mathbf{K}_{IJ}^{ss} = \int_{\Omega}(\mathbf{B}_{sI}^T\mathbf{D}\mathbf{B}_{sJ} + \mathbf{B}_{wI}^T(1-n)^2/n\,E_w\mathbf{B}_{wJ})d\Omega \qquad \mathbf{K}_{IJ}^{ww} = \int_{\Omega}\mathbf{B}_{wI}^T nE_w\mathbf{B}_{wJ}d\Omega \tag{3.10}$$

$$\mathbf{K}_{IJ}^{sw} = \int_{\Omega}\mathbf{B}_{wI}^T(1-n)E_w\mathbf{B}_{wJ}d\Omega \qquad \mathbf{K}_{IJ}^{ws} = \int_{\Omega}\mathbf{B}_{wI}^T(1-n)E_w\mathbf{B}_{wJ}d\Omega \tag{3.11}$$

$$\mathbf{B}_{sI} = \mathbf{L}_s\mathbf{\Phi}_I \qquad \mathbf{B}_{wI} = \mathbf{L}_w\mathbf{\Phi}_I \tag{3.12}$$

Finally, the external nodal forces are given by

$$\mathbf{F}_I^{S} = \int_{\Gamma_N^s}\mathbf{\Phi}_I^T\bar{\mathbf{t}}d\Gamma \qquad \mathbf{F}_I^{w} = \int_{\Gamma_N^w}\mathbf{\Phi}_I^T\mathbf{n}n\bar{P}d\Gamma \tag{3.13}$$

Eqn.3.6 nd Eqn.3.7 can be viewed as the system equations of the Ith field node. Assembling all system equations of all field nodes based on the global numbering system, we can obtain the final global system equations and consistent-mass matrix, which leads to time-consuming algebra equation sets solving at each time step. Here, we call this method as the conventional RPIM.

4. DECOUPLED RPIM

To guarantee the accuracy in simulating wave motion, the nodal spacing is required to be substantially smaller than the smallest wavelength considered. Thus, the spatial variations of acceleration and mass density can be ignored in support domain, that means

$$\ddot{\mathbf{u}}_J = \ddot{\mathbf{u}}_I \qquad \ddot{\mathbf{U}}_J = \ddot{\mathbf{U}}_I \qquad (J = 1,\cdots,N) \tag{4.1}$$

Substituting Eqn.4.1 into Eqn. 3.7 and Eqn.3.8, we have

$$\ddot{\mathbf{u}}_I\mathbf{M}_I^{s} + \sum_{J=1}^{N}\mathbf{K}_{IJ}^{ss}\mathbf{u}_J + \sum_{J=1}^{N}\mathbf{K}_{IJ}^{sw}\mathbf{U}_J + \sum_{J=1}^{N}\mathbf{C}_{IJ}^{ss}\dot{\mathbf{u}}_J + \sum_{J=1}^{N}\mathbf{C}_{IJ}^{sw}\dot{\mathbf{U}}_J = \mathbf{F}_I^{s} \tag{4.2}$$

$$\ddot{\mathbf{U}}_I\mathbf{M}_I^{w} + \sum_{J=1}^{N}\mathbf{K}_{IJ}^{ws}\mathbf{u}_J + \sum_{J=1}^{N}\mathbf{K}_{IJ}^{ww}\mathbf{U}_J + \sum_{J=1}^{N}\mathbf{C}_{IJ}^{ws}\dot{\mathbf{u}}_J + \sum_{J=1}^{N}\mathbf{C}_{IJ}^{ww}\dot{\mathbf{U}}_J = \mathbf{F}_I^{w} \tag{4.3}$$

where，

$$\mathbf{M}_I^s = \sum_{J=1}^{N} \mathbf{M}_{IJ}^s = \begin{bmatrix} M_I^s & 0 & 0 \\ 0 & M_I^s & 0 \\ 0 & 0 & M_I^s \end{bmatrix} \qquad \mathbf{M}_I^w = \sum_{J=1}^{N} \mathbf{M}_{IJ}^w = \begin{bmatrix} M_I^w & 0 & 0 \\ 0 & M_I^w & 0 \\ 0 & 0 & M_I^w \end{bmatrix} \tag{4.4}$$

Time integration of the semi-discrete finite element Eqn.4.2 and Eqn.4.3 can be performed by explicit procedure proposed by Li et al.(1992), we can obtain

$$\mathbf{u}_I^{p+1} = \mathbf{u}_I^p + \Delta t \dot{\mathbf{u}}_I^p - \frac{\Delta t^2}{2} \frac{1}{M_I^s} \left(\sum_{J=1}^{N} \mathbf{K}_{IJ}^{ss} \mathbf{u}_J^p + \sum_{J=1}^{N} \mathbf{K}_{IJ}^{sw} \mathbf{U}_J^p + \sum_{J=1}^{N} \mathbf{C}_{IJ}^{ss} \dot{\mathbf{u}}_J^p + \sum_{J=1}^{N} \mathbf{C}_{IJ}^{sw} \dot{\mathbf{U}}_J^p - \mathbf{F}_I^{sp} \right) \tag{4.5}$$

$$\mathbf{U}_I^{p+1} = \mathbf{U}_I^p + \Delta t \dot{\mathbf{U}}_I^p - \frac{\Delta t^2}{2} \frac{1}{M_I^w} \left(\sum_{J=1}^{N} \mathbf{K}_{IJ}^{ws} \mathbf{u}_J^p + \sum_{J=1}^{N} \mathbf{K}_{IJ}^{ww} \mathbf{U}_J^p + \sum_{J=1}^{N} \mathbf{C}_{IJ}^{ws} \dot{\mathbf{u}}_J^p + \sum_{J=1}^{N} \mathbf{C}_{IJ}^{ww} \dot{\mathbf{U}}_J^p - \mathbf{F}_I^{wp} \right) \tag{4.6}$$

where, Δt is the time step, $\mathbf{u}_I^p$ ($\mathbf{U}_I^p$) and $\dot{\mathbf{u}}_I^p$ ($\dot{\mathbf{U}}_I^p$) are the solid (fluid) displacement and velocity vectors of the Ith node at time $p\Delta t$ respectively.

$$\begin{aligned} \dot{\mathbf{u}}_I^{p+1} = \dot{\mathbf{u}}_I^p &- \frac{\Delta t}{2M_I^s} \left[\sum_{J=1}^{N} \mathbf{K}_{IJ}^{ss} (\mathbf{u}_J^{p+1} + \mathbf{u}_J^p) + \sum_{J=1}^{N} \mathbf{K}_{IJ}^{sw} (\mathbf{U}_J^{p+1} + \mathbf{U}_J^p) + \frac{2}{\Delta t} \sum_{J=1}^{N} \mathbf{C}_{IJ}^{ss} (\mathbf{u}_J^{p+1} - \mathbf{u}_J^p) \right] \\ &- \frac{\Delta t}{2M_I^s} \left[\frac{2}{\Delta t} \sum_{J=1}^{N} \mathbf{C}_{IJ}^{sw} (\mathbf{U}_J^{p+1} - \mathbf{U}_J^p) - (\mathbf{F}_I^{s(p+1)} + \mathbf{F}_I^{sp}) \right] \end{aligned} \tag{4.7}$$

$$\begin{aligned} \dot{\mathbf{U}}_I^{p+1} = \dot{\mathbf{U}}_I^p &- \frac{\Delta t}{2M_I^w} \left[\sum_{J=1}^{N} \mathbf{K}_{IJ}^{ws} (\mathbf{u}_J^{p+1} + \mathbf{u}_J^p) + \sum_{J=1}^{N} \mathbf{K}_{IJ}^{ww} (\mathbf{U}_J^{p+1} + \mathbf{U}_J^p) + \frac{2}{\Delta t} \sum_{J=1}^{N} \mathbf{C}_{IJ}^{ws} (\mathbf{u}_J^{p+1} - \mathbf{u}_J^p) \right] \\ &- \frac{\Delta t}{2M_I^w} \left[\frac{2}{\Delta t} \sum_{J=1}^{N} \mathbf{C}_{IJ}^{ww} (\mathbf{U}_J^{p+1} - \mathbf{U}_J^p) - (\mathbf{F}_I^{w(p+1)} + \mathbf{F}_I^{wp}) \right] \end{aligned} \tag{4.8}$$

Using Eqns.4.5-4.8, we can obtain the displacements and velocities of all field nodes without solving algebra set of equations.

5. NUMERICAL EXAMPLES

Consider a plane strain problem in two-dimensional domain as shown in Fig.1. The boundaries are all fully fixed and impermeable. Suppose that a point force $F(t)$ acts on the solid skeleton at point (1.0,1.0) along y direction. The function $F(t)$ is defined as

$$F(t) = \begin{cases} \sin(8\pi t), 0 \le t \le 0.125 \\ 0, t > 0.125 \end{cases} \tag{5.1}$$

The material constants used in computation are : $E_s = 2.5\times10^6 \text{kN/m}^2$, $v = 0.3$, $E_w = 2.5\times10^5 \text{kN/m}^2$, $k = 2.5\times10^{-2} \text{m/s}$, $\rho_s = 3.0\times10^3 \text{kg/m}^3$, $\rho_w = 1.0\times10^3 \text{kg/m}^3$, $n = 0.4$. The dimension of the model is $2\text{m}\times2\text{m}$ and the domain is represented by regularly distributed $441(21\times21)$ field nodes and irregularly distributed 441 field nodes respectively as plotted in Fig.2. A total of $100\,(10\times10)$ regularly rectangular background cells are used for the numerical integrations. In each rectangular background cell, 16 Gauss points are employed. The MQ-RBF is used in RPIM and the shape parameters used are $q = 1.03$, $\alpha_c = 4.0$ and $d_c = 0.1$. The linear polynomial terms are added in the RPIM-MQ. The dimensionless size of the support domain is $\alpha_s = 1.5$. For comparison, the conventional RPIM, the conventional FEM and decoupled FEM results are computed. Here, The conventional method refers to which uses consistent mass and Newmark time integration, and the decoupled method refers to which uses lumped mass and explicit time integration in this paper. The integration time step is $\Delta t = 0.001s$.

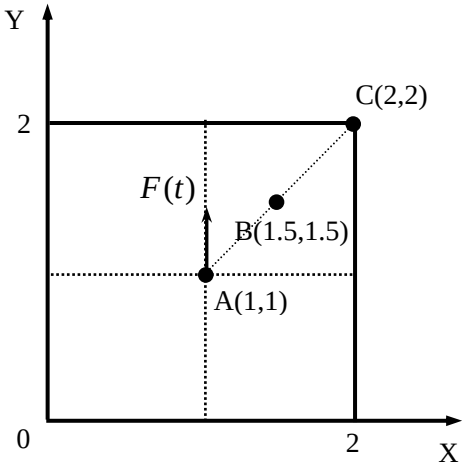

Figure 1 Two-dimensional point source model

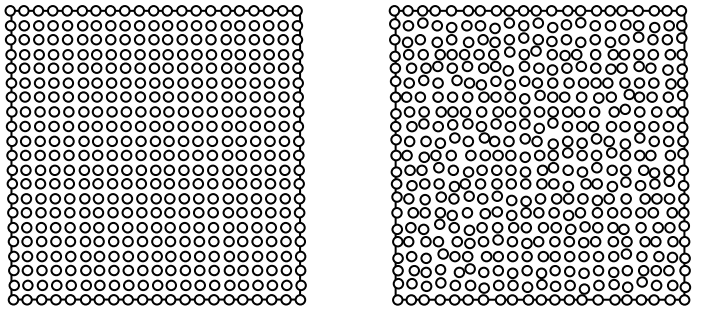

(a) regular nodes distribution b) irregular nodes distribution

Figure 2 Nodal arrangements for the plane strain problem

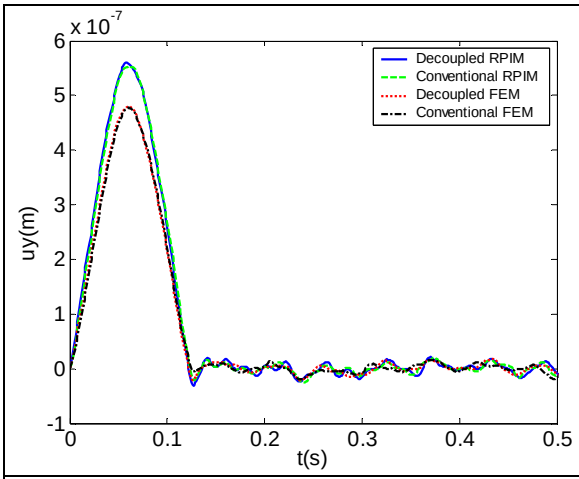

Figure 3 Displacement of solid phase in y direction at the point (1.0,1.0)

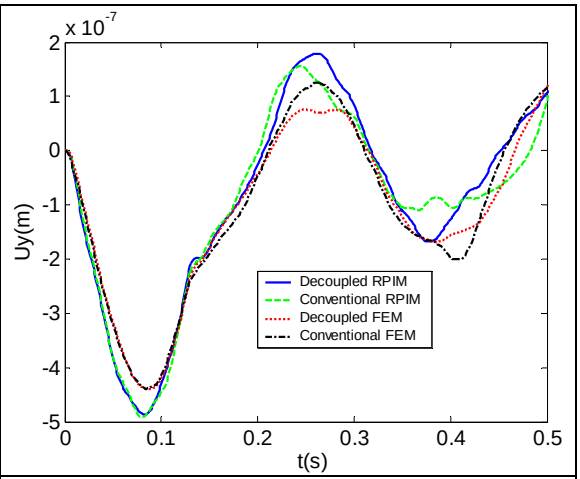

Figure 4 Displacement of fluid phase in y direction at the point (1.0,1.0)

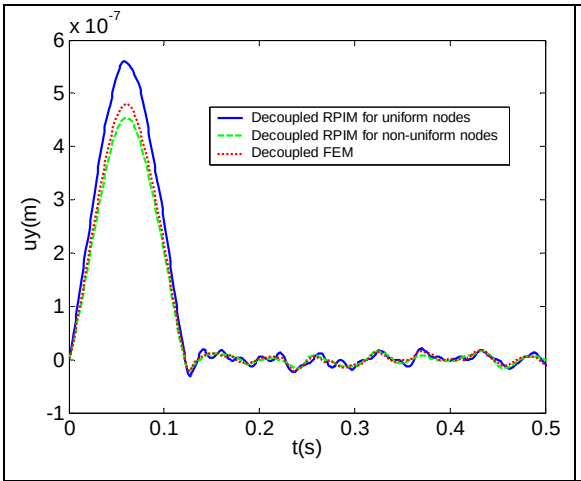

Figure 5 Displacement of solid phase in y direction at the point (1.0,1.0)

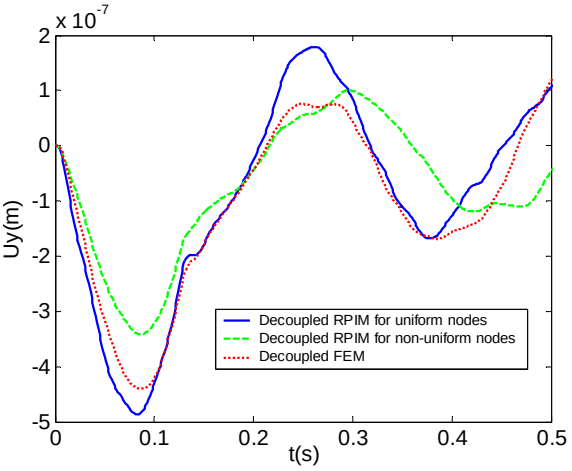

Figure 6 Displacement of fluid phase in y direction at the point (1.0,1.0)

The displacements at points A(1.0,1.0) for uniform nodal distribution case are plotted in Figure 3 and Figure 4, with the solid line denoting the results of the decoupled RPIM, the dash line representing the results of the conventional RPIM, the dot line denoting the solutions of the decoupled FEM, and the dash-dot line representing the solutions of the conventional FEM. For symmetry, the displacements in x direction at point A(1.0,1.0) is zero. From the results, it is found that the agreement between the decoupled RPIM and conventional RPIM solutions are satisfactory before $t = 1.2s$ and not so well satisfactory after $t = 1.2s$. The same phenomenon can be found between the decoupled FEM and conventional FEM solutions. This may result from the different algorithm damping of the time integration schemes used in decoupled method and conventional method in this study. The discrepancy may be reduced if time integration schemes with the same algorithm damping are used in decoupled method and conventional method. The deviations between the conventional FEM and conventional RPIM solutions (or between the decoupled FEM and decoupled RPIM solutions) are due to the different accuracy of FEM and RPIM in the case of this study. On the whole, the proposed decoupled RPIM has the comparable accuracy with the conventional RPIM and FEM.

The results for non-uniform nodal distribution case are plotted in Figure 5 and Figure 6. From these figures, it can be found that the effect of nodal distribution on displacements of fluid phase is larger than that on displacements of solid phase. Compared with FEM, the accuracy of decoupled RPIM is acceptable for irregular nodal distribution.

The computational costs of different methods are given in Table 5.1. It can be seen that the CPU time of the conventional RPIM is about 88 times as much as that of the decoupled RPIM, and the CPU time of the conventional FEM with 400 elements is about 77 times as mush as that of the decoupled RPIM. Using the same mass form and time integration, the RPIM has worse computational efficiency than FEM, that is because the node number within a support domain in RPIM is generally greater than the node number of an element in FEM and the shape function of RPIM is more complex than that of FEM. The computational cost of the conventional RPIM increases more rapidly than that of decoupled RPIM as the degree of freedoms increases. Thus, it can be predicted that the high efficiency of the decoupled RPIM is more obvious in larger model.

Table 5.1 Computational cost of different methods

Method	Number of nodes	CPU time (seconds)
Decoupled RPIM	441	649.8
Conventional RPIM	441	57600.9
Decoupled FEM	441(400 elmemts)	584.0
Conventional FEM	441(400 elmemts)	50400.8

6. CONCLUSIONS

An efficient meshless method, namely, the decoupled RPIM is developed to analyze the transient response of saturated porous elastic media. This method employs the radial point interpolation to construct the meshless shape functions. The discrete equations for saturated porous elastic media are obtained using the global weak-forms, and a lumped-mass RPIM is derived by meeting the requirements of accuracy in wave simulation. Combing the lumped-mass RPIM with explicit time integration scheme leads to the decoupled discrete equations, which can be solved one by one at one time step avoiding solving algebra equation sets. The RPIM shape functions possess the Kronecker delta function property, thus no additional treatment is needed to impose essential boundary conditions. Numerical examples show that the decoupled RPIM possesses comparable accuracy with the conventional RPIM and FEM, and is more efficient than the conventional RPIM.

Acknowledgments

This study was supported by the Natural Science Foundation of China (50508016) and National Basic Research Program of China (2007CB714201).

REFERENCES

[1] Atluri,S.N.,Zhu,T.(1998). A new meshless local Petrov-Galerkin (MLPG) approach in computational mechanics. *Computational Mechanics* **22**,117-127.
[2] Belytschko,T., Lu,Y.Y., Gu,L.(1994). Element-free Galerkin methods. *International Journal for Numerical Methods in Engineering* **37**,229-256.
[3] Biot,M.A.(1941).General theory of three-dimensional consolidation. *Journal of Applied Physics* **12**,155-164.
[4] Diebels,S.,Ehlers,W.(1996).Dynamic analysis of a fully saturated porous medium accounting for geometrical and material non-linearities. *International Journal for Numerical Methods in Engineering* **39**,81-97.
[5] Ghaboussi,J.,Wilson,E.L.(1972).Variational formulation of dynamics of fluid-saturated porous elastic solids. *Journal of the Engineering Mechanics Division, ASCE EM4*,947-963.
[6] Gingold,R.A., Moragham,J.J.(1977).Smooth particle hydrodynamics:Theory and applications to non spherical stars. *Monthly Notices of the Royal Astronomical Society* **181**,375-389.
[7] Gu,Y.T., Liu,G.R.(2001). A meshless Local Petrov-Galerkin (MLPG) method for free and forced vibration analyses for solids. *Computational Mechanics* **27:3**,188-198.
[8] Gu,Y.T., Liu,G.R.(2001). A local point interpolation method for static and dynamic analysis of thin beams. *Computer Methods in Applied Mechanics and Engineering* **190**,5515-5528.
[9] Huang,M.S.,Yue, Z.Q.,Tham,L.G.et al.(2004). On the stable finite element procedures for dynamic problems of saturated porous media. *International Journal for Numerical Methods in Engineering* **61:9**,1421-1450.
[10] Karim,M.R., Nogami,T., Wang J.G.(2002). Analysis of transient response of saturated porous elastic soil under cyclic loading using element-free Galerkin method. *International Journal of Solids and Structures* **39**,6011-6033.
[11] Li,X.J., Liao,Z.P., Du,X.L.(1992).A explicit integration procedure for dynamic system with damping.In:Engineering Mechanics(in Chinese),Science Press,Beijing.
[12] Liao,Z. P.(1999). Dynamic interaction of natural and man-made structures with earth medium. *Earthquake Research in China* **13:3**,367-408.
[13] Liu,G.R., Gu,Y.T.(2001). A local radial point interpolation method(LRPIM)for free vibration analyses of 2-D solids. *Journal of Sound and Vibration* **246:1**,29-46.
[14] Liu,W.K., Jun,S., Zhang,Y.(1995).Reproducing kernel particle methods. *International Journal for Numerical Methods in Engineering* **20**,1081-1106.
[15] Men,F.L.(1982). On wave propagation in fluid-saturated porous media, In: Soil Dynamics and Earthquake Engineering Conference. Spain,Vol.1.
[16] Nayroles,B., Touzot,G., Villon,P.(1992). Generalizing the finite element method:diffuse approximation and diffuse elements. *Computational Mechanics* **10**,307-318.
[17] Prevost J.H.(1985).Wave propagation in fluid-saturated porous media: an efficient finite element procedure. *Soil Dynamics and Earthquake Engineering* **4:4**,183-201.
[18] Sandhu R. S., Hong S. J.(1987).Dynamics of fluid-saturated soils variational formulation. *International Journal for Numerical and Analytical Methods in Geomechanics* **11:1**,241-255.
[19] Wang J.G., Liu G.R., Wu Y.G.(2001)A point interpolation method for simulation dissipation process of consolidation. *Computer Methods in Applied Mechanics and Engineering* **190**,5907-5922.
[20] Wang J.G., Liu G.R.(2001). A point interpolation meshless method based on radial basis functions.*International Journal for Numerical Methods in Engineering* **54:1**,1623-1648.
[21] Wang J.G., Liu G.R., Lin P.(2002). Numerical analysis of Biot's consolidation process by radial point interpolation method.*International Journal of Solids and Structures*, **39**,1557-1573.
[22] Yiagos,A.N.,Prevost,J.H.(1991). Two-phase elasto-plastic seismic response of earth dams: application. *Soil Dynamics and Earthquake Engineering* **10:7,**371-381.
[23] Zienkiewicz,O.C.,Shiomi,T.(1984). Dynamic behaviour of saturated porous media; the generalized biot formulation and its numerical solution. *Journal for Numerical and Analytical Methods in Geomechanics* **8:1,**71-96**.**